Supporting Information for "Four Dimensional Paleomagnetic Dataset: Late Neogene paleodirection and paleointensity Results from the Erebus Volcanic Province, Antarctica"

H.A. Asefaw[1], L. Tauxe[1], A.A.P. Koppers [2], H. Staudigel[1]

[1]Scripps Institution of Oceanography, University of California

[2]College of Earth, Ocean and Atmospheric Sciences

Contents of this file

1. Figures S1 to S5

2. Table S1 to S2

New Site	Combined Sites
mc1301	mc1012, mc1203
mc1302	mc1013, mc1204
mc1303	mc1026, mc1129
mc1304	mc1049, mc1104
mc1305	mc1050, mc1105
mc1306	mc1161, mc1162
mc1307	mc1166, mc1219

Table S1. Several lava flows that were considered separate sites from the original study recover identical paleodirections. Field examination suggests that these sites likely sample the same event, so we combined the original sites, listed in the combined sites column, into a single site.

Table S2. Plateau age, normal isochron age, inverse isochron age, and total fusion age results from the $^{40}Ar/^{39}Ar$ incremental heating method used for geochronology.

Figure S1. A representative outcrop containing the original drill cores of Lawrence et al. 2009 sampled from the interior of the lava flow and the hand samples collected for this study from the lava flow top.

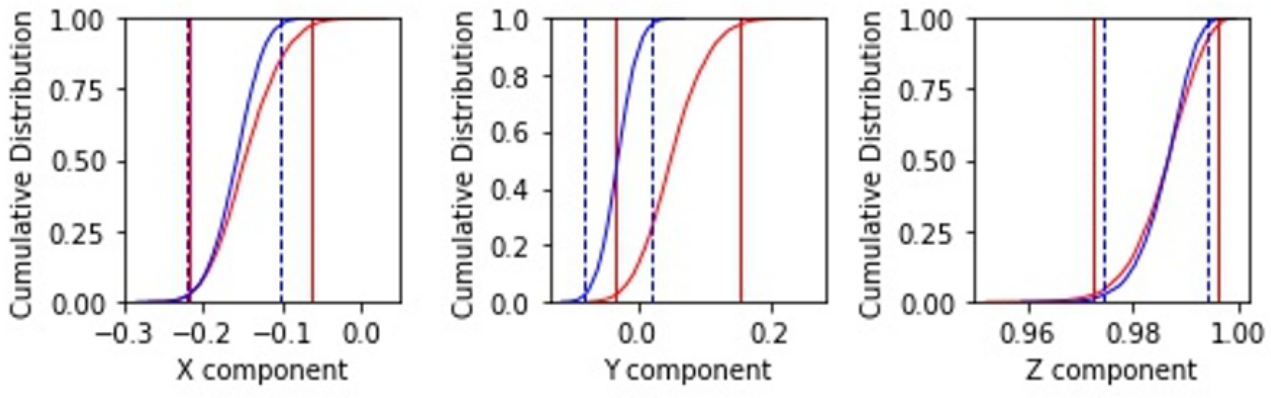

Figure S2. The results of the bootstrap reversal test applied to the normal and reverse directions. A bootstrap approach is applied by resampling 1000 normal directions, calculating their mean direction and then repeating this procedure 1000 times. The results of the mean normal directions (blue) and the mean reverse directions (red) are displayed as cumulative distribution functions of the x-component (left), y-component (center), and z-component(right) of the mean directions. The corresponding 95% confidence bounds for the normal (vertical red lines) and reverse (vertical blue lines) directions.

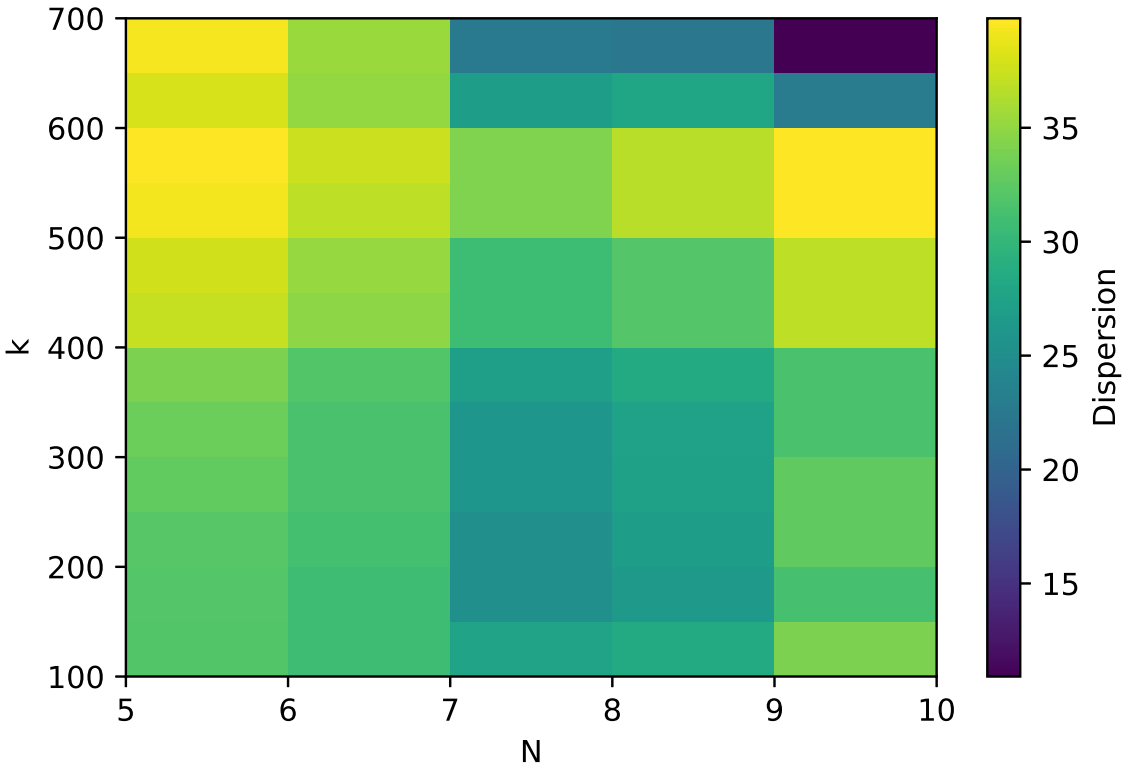

Figure S3. A heat map of dispersion calculated from our combined normal and reverse polarity directions that was filtered by different combinations of N, the number of cores, and k, the precision parameter.

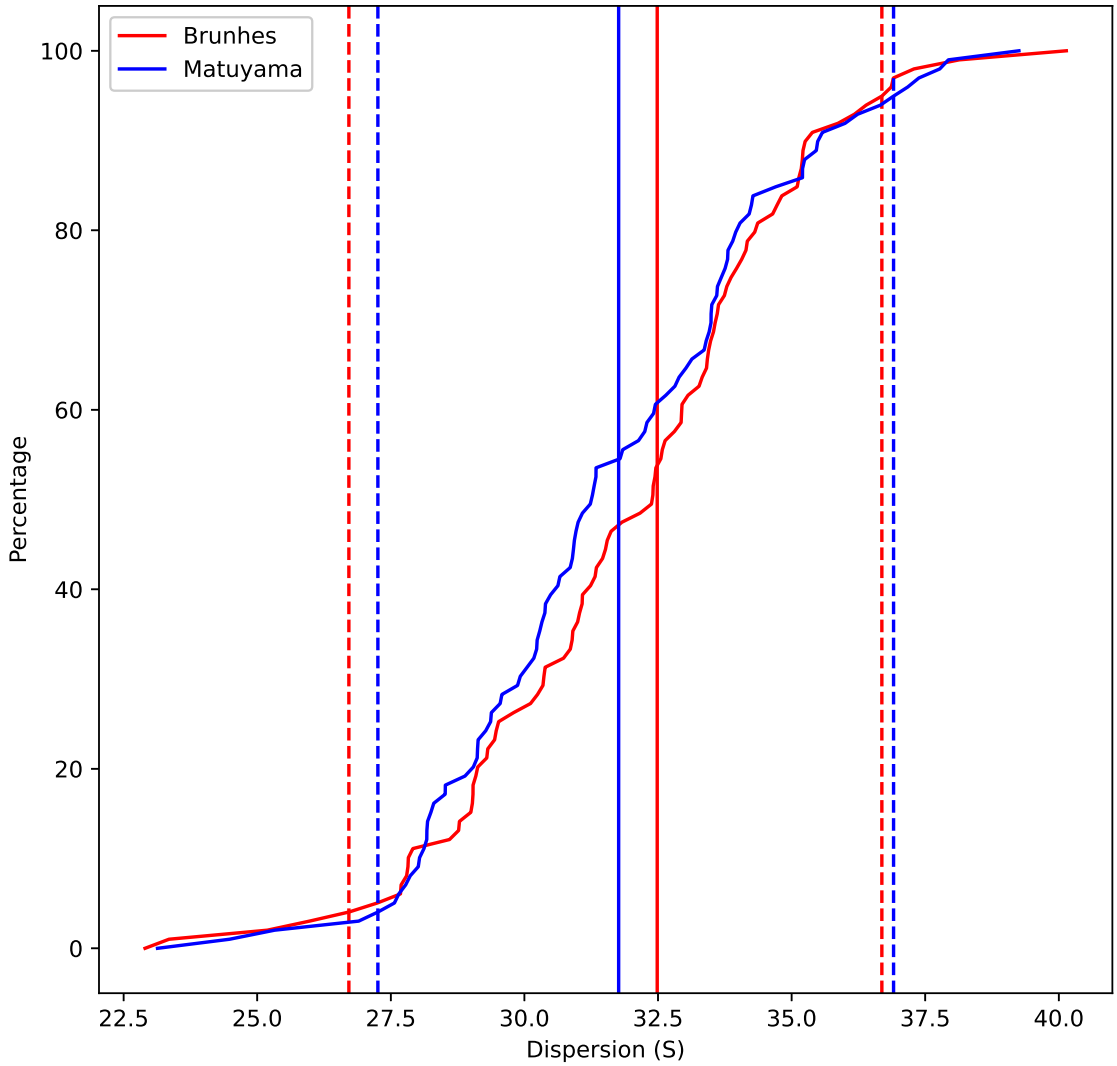

Figure S4. The CDF (cumulative distribution function) of dispersion (S) for 1000 bootstrap subsets of our Brunhes (red) and Maytuyama (blue) datasets. The 95% confidence bounds are marked as vertical dashed lines.

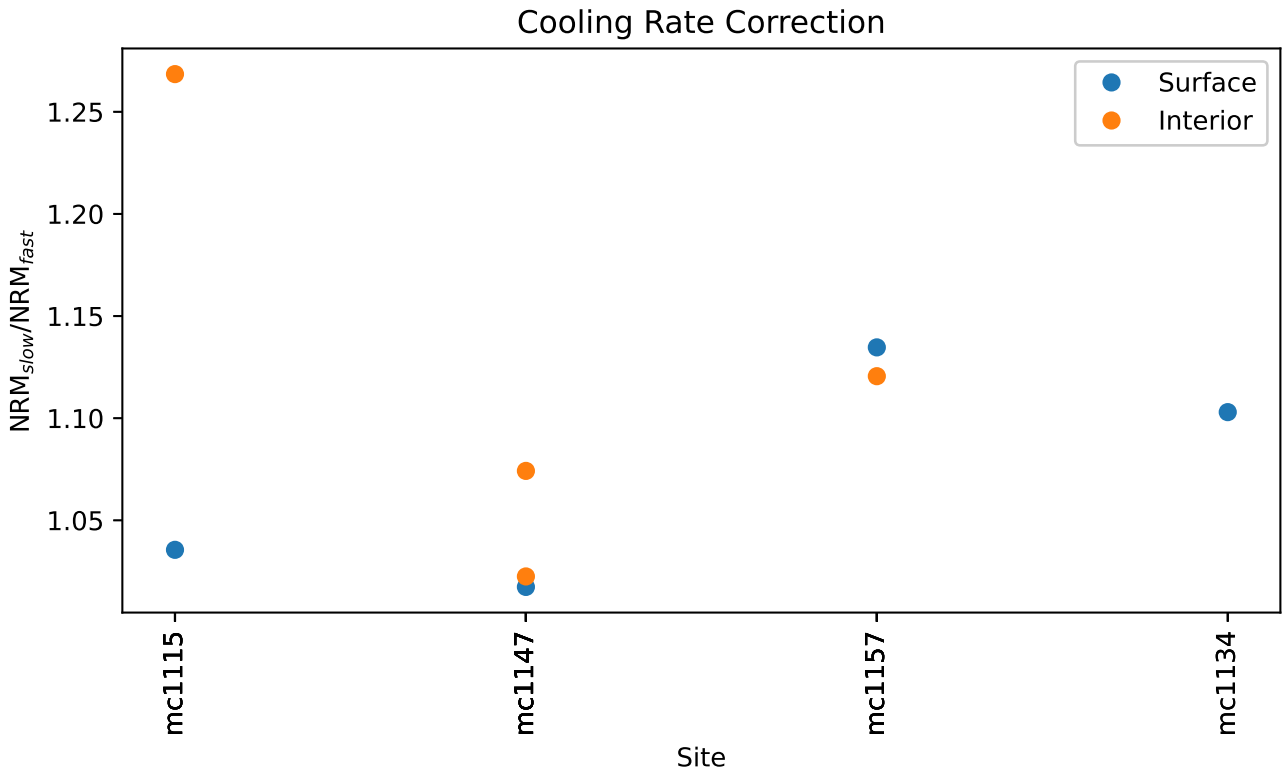

Figure S5. The results of the cooling rate experiment. Each specimen requires a cooling rate correction ranging from 2% to 27%, but the correction for the specimen from the interiors equals (mc1157) or exceeds (mc1115, mc1147) the cooling rate correction required for the specimen from the surface of the same lava flow.

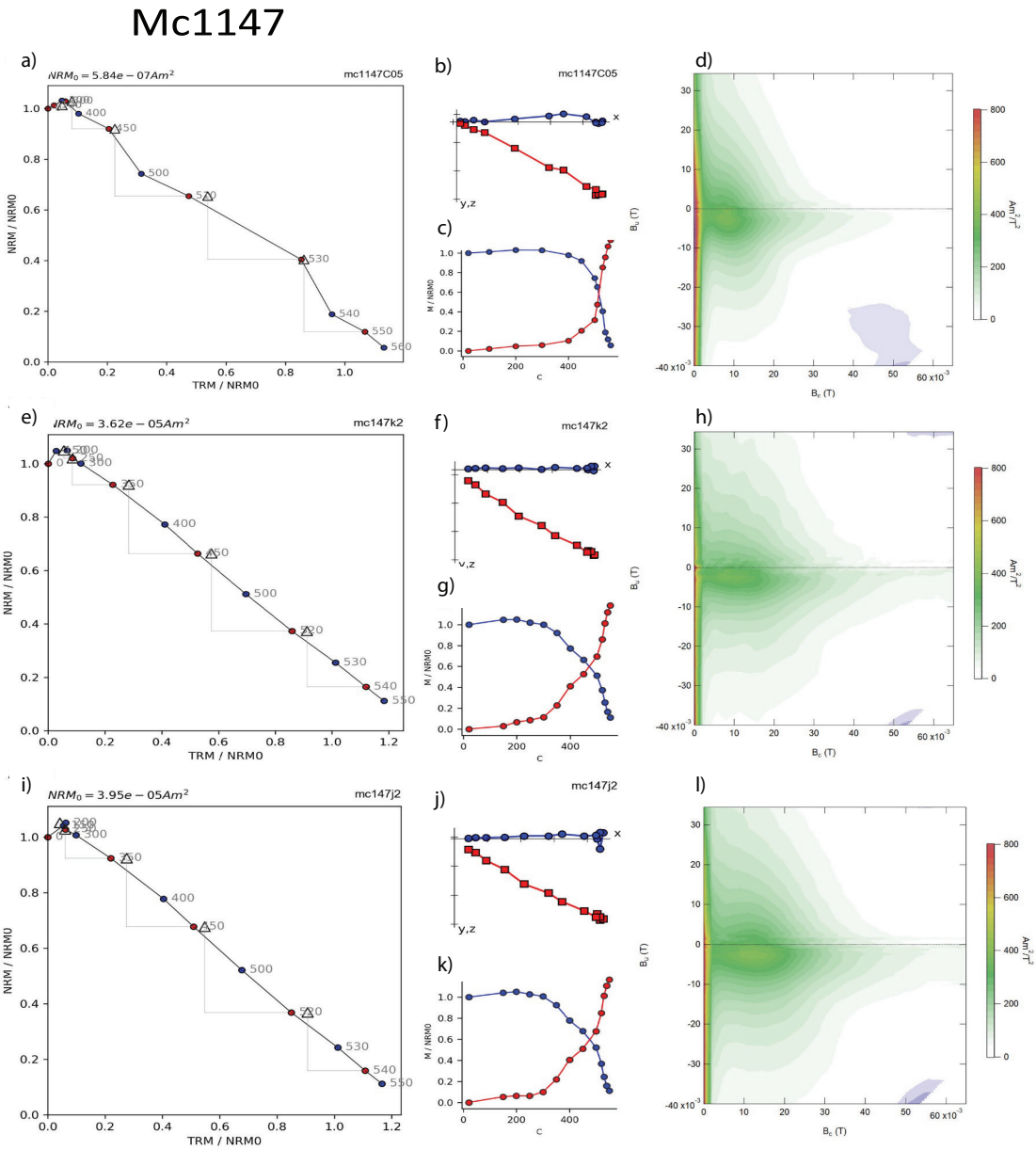

Figure S6. Arai diagram (a,e,i), zijderveld diagram (b, f, j), MT curve (c,g, k), and FORC diagrams (d,h,l) for samples from site mc1147 that passed CCRIT. Specimen mc1147C05 (a - d) was sampled from the lava flow top and yielded a 25.8T paleointensity; mc147k2 (e-h) was collected from the lava flow interior and estimated a 21.1T paleointensity; mc147j2 (i-l) was sampled from the lava flow interior and yielded a 21.3T

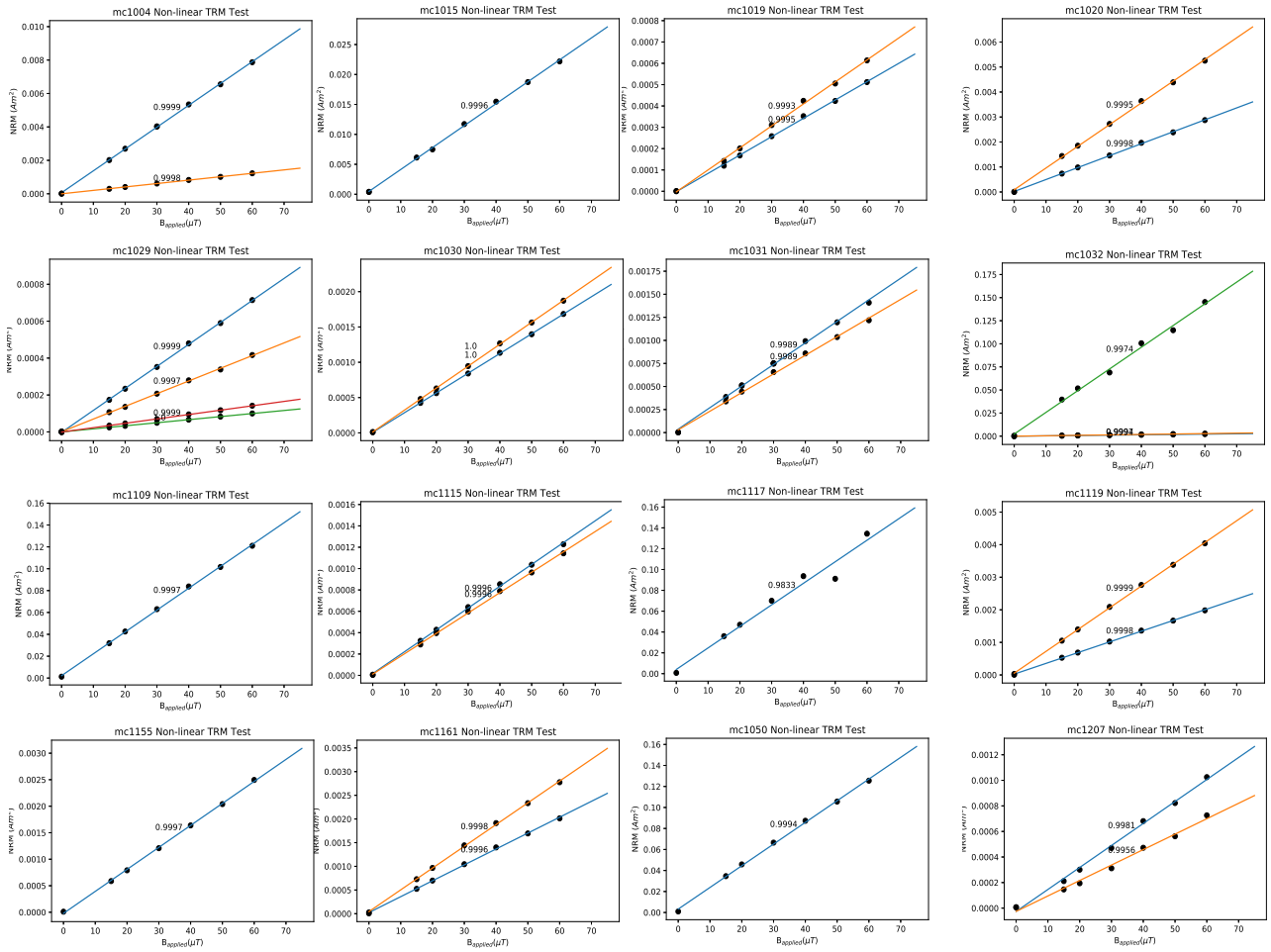

Figure S7. Results of the non-linear TRM acquisition test. Specimen are grouped by site, each line is a successful specimen from that site. The best fit line for each specimen is plotted along with its correlation coefficient.